

# Characterizing the delocalized-localized Anderson phase transition based on the system's response to boundary conditions

Mohammad Pouranvari<sup>1\*</sup>

<sup>1\*</sup> Department of Solid-State Physics, Faculty of Science, University of Mazandaran, Babolsar, 4741613534, Iran .

Corresponding author(s). E-mail(s): [m.pouranvari@umz.ac.ir](mailto:m.pouranvari@umz.ac.ir);

## Abstract

A new characterization of the Anderson phase transition, based on the response of the system to the boundary conditions is introduced. We change the boundary conditions from periodic to antiperiodic and look for its effects on the eigenstate of the system. To characterize these effects, we use the overlap of the states. In particular, we numerically calculate the overlap between the ground-state of the system with periodic and antiperiodic boundary conditions in one-dimensional models with delocalized-localized phase transitions. We observe that the overlap is close to one in the localized phase, and it gets appreciably smaller in the delocalized phase. In addition, in models with mobility edges, we calculate the overlaps between single-particle eigenstate with periodic and antiperiodic boundary conditions to characterize the entire spectrum. By this single-particle overlap, we can locate the mobility edges between delocalized and localized states.

## 1 Introduction

Characterizing phases and phase transitions is one of the main goals of condensed matter physics. Introducing a new method to understand the nature of the phases, also to locate the phase transition point are always the essential parts of the current research. In general, the classical interpretations are enough for a description of the system phases and for the phase transitions. The story is different for a zero-temperature phase transition, where quantum fluctuations become essential and dominate thermal fluctuations. Among quantum phase transitions, Anderson phase transition[1] between a delocalized and a localized phase has attracted much attentions[2–4]. In this form of phase transition, disorder plays the central role.

For an ideal clean system, which is translationally invariant, the Bloch waves propagate through the entire system, and thus system's eigenstate is extended, and the system is in the metallic phase. Introducing the disorder in the system, which change the Physics of the system. Interferences of the scattered waves of the disorders can be destructive and make the system localized. This localization depends on the dimension of the system. In one- and two-dimensional systems, any infinitesimal disorder makes the system localized[5]. On the other hand, in the three-dimensional systems, we have a phase transition between delocalized and localized phases as we increase the disorder strength. For a small disorder strength, the state of the system is still delocalized, but when the disorder strength is

larger than a critical value, it will become localized in a small part of the system [6, 7] (this critical value depends on the randomness distribution). There are also one-dimensional models with a *correlated* disorder that exhibit phase transitions between delocalized and localized phases[5, 8, 9]. On the other hand, Hamiltonian's size of these one-dimensional models correspond to matrices that increases linearly with the system size. Since they represent the same nature of the Anderson localization, compared to those two- and three-dimensional models with Anderson phase transition, they are more suitable for numerical calculations.

People use different quantities to characterize the transition between delocalized and localized phases. Since the eigenstate of the system at the Fermi level shows the tendency of the material to conduct an electron, one of the obvious characterizations is to measure the extent of the Fermi level eigenstate. To quantify how much an eigenstate of the system  $\psi$  is extended, people use the participation ratio:

$$\text{PR} = \frac{1}{\sum_{i=1}^N |\psi_i|^4}, \quad (1)$$

( $N$  is the system size) where for a normalized eigenstate,  $\psi_i$  is the probability amplitude at each site  $i$ . In the delocalized phase, where the system is extended in the entire system,  $\psi_i$  approaches  $1/\sqrt{N}$ , and thus PR goes to  $N$ . On the other hand, in the localized phase where the state of the system is localized at a few sites, PR approaches to  $O(1)$ . The next candidate would be entanglement. In the delocalized phase, we expect a larger correlation in the system than in the localized phase. Thus, the amount of the entanglement is larger in the delocalized phase. Thus, the system entanglement properties can locate the phase transition point[10–15].

Besides the system's eigenstate, looking at the system's energy eigenvalues is also informative. Level spacing (defined as  $\Delta_n = E_{n+1} - E_n$  as a difference between the adjacent energies  $\{E\}$ ) and their distributions are another way to characterize a delocalized from a localized phases[16]. That stems from the fact that, in contrast to the localized phase, the energy spectrum is doubly degenerated in the delocalized phase, and thus there is a gap between even-odd and odd-even

level spacing[17, 18]. Moreover, the ratio of the level spacing:

$$r_n = \frac{\min(\Delta_n, \Delta_{n+1})}{\max(\Delta_n, \Delta_{n+1})}, \quad (2)$$

is also useful. In the delocalized phase, where the energy spectrum has a Wigner-Dyson distribution, the disorder average of  $r_n$  approaches to  $\approx 0.53$ , and in the localized phase with Poisson statistics of the energy spectrum, it goes to  $\approx 0.386$ . Thus, people use the ratio of the level spacing to distinguish delocalized from localized phases[19–21].

The response of a system to a local quench is also another characterization. A measure of this response is fidelity. If we consider  $|G\rangle$  as the ground state of the system without a local quench and  $|G'\rangle$  as the ground state of the system with a local quench, then the fidelity is the overlap  $F = |\langle G|G'\rangle|$  of these two states [22–27]. This overlap goes to zero in a power-law fashion ( $F \sim N^{-\gamma}$ ) in the delocalized phase, the so-called Anderson orthogonality catastrophe [28]. While, it decays exponentially in the localized phase ( $F \sim e^{-\beta N}$ ); where  $\gamma$  and  $\beta$  depend on the disorder strength[28–32].

To characterize the delocalized-localized phase transition, we can also look at the system's behavior upon the change in the boundary conditions[33, 34]. For an extended eigenstate, the change in the boundary conditions is seen by the eigenstate, so it is reflected in the corresponding eigenenergy. In contrast, in a localized eigenstate, where the amplitude of the wavefunction is approximately non-zero for some finite number of sites only, the change in the boundary conditions is not seen by the eigenstate. Thus, there will be no change in the corresponding eigenenergy. On this subject, Ref. [35] used the shift in the eigenenergy when the boundary conditions are changed from periodic to antiperiodic to characterize the delocalized-localized phase transition. In the same way, in Ref [36], we change the boundary conditions from periodic to antiperiodic and calculate the shift in the entanglement spectrum, and also the shift in the entanglement entropy. We observe that the entanglement properties of the system are sensitive to the boundary conditions in the delocalized phase, and become insensitive in

the localized phase. Thus, the shift in the entanglement entropy and spectrum can be used to characterize the Anderson phase transition. Similarly, we studied the change in the single-particle density matrix for a many-body system, when boundary conditions are changed from periodic to antiperiodic in Ref [37]. We observed that the shift in the spectrum of the single-particle density matrix is non-vanishing in the delocalized phase, and it goes to zero in the localized phase; it is thus a characterization of the many-body localization.

In this paper, we look for the *direct* effect of the change in the boundary conditions on the system's *state* (We know that we can directly observe the eigenstate of the system in experiment[38]). In practice, we use the concept of the fidelity regarding the states with different boundary conditions. In particular, we calculate the overlap between the state of the system with the periodic boundary conditions (PBC) and the corresponding state of the system with antiperiodic boundary conditions (APBC) to characterize their similarity. We expect that the overlap (between the state of the system with PBC and APBC) becomes unity in the localized phase and it becomes smaller than one in the delocalized phase. In this regard, we expect that the overlap distinguishes a localized from a delocalized phases.

In free fermion models, to obtain the ground state of the system corresponding to a Fermi energy, we do the followings. We fill single-particle eigenstates of the system from the lowest eigenenergy up to the Fermi level, and the many-body ground state of the system is the Slater determinant of these single-particle eigenstates. To observe and calculate the similarity between many-body eigenstates, we can thus calculate the overlap between the many-body ground state of the system with PBC and APBC. Besides, we can also look at the overlaps of the single-particle eigenstates separately—those eigenstates that build the many-body state of the system. In this regard, we calculate the many-body ground states of the system with PBC and APBC, then we obtain their overlap, and we call it ground-state overlap (GSO). In addition, we calculate the single-particle eigenstates of the system with PBC and APBC, and we call their corresponding overlaps single-particle overlap (SPO). We show that the behavior of the GSO and SPO are different in the delocalized and the localized

phases. Thus, we utilize them to characterize the delocalized-localized phase transition.

The remainder of this paper is as follows. In section 2 we explain the models we employ in this paper to verify our ideas. Also the calculations methods for the SPO and GSO are explained. Section 3 is devoted to our numerical calculations, where we present the results for the SPO and GSO for the models. We also show how they can be used as phase transition characterization. We conclude the paper in section 4 with some suggestions for future works.

## 2 Method and models

We work with one-dimensional free fermion tight-binding models with the following Hamiltonian:

$$H = -t \sum_{i=1}^N (c_i^\dagger c_{i+1} + c_{i+1}^\dagger c_i) + \sum_{i=1}^N \varepsilon_i c_i^\dagger c_i, \quad (3)$$

where,  $c_i (c_i^\dagger)$  is the annihilation (creation) operator for the  $i$ th site.  $N$  is the number of sites in the system. The amplitude of the nearest-neighbor hopping is  $t$ , and we set it to be 1 as the energy scale. The models we use in this paper are determined by their on-site energies  $\{\varepsilon\}$ . One of the models is the random dimer (RD) model, where  $\varepsilon_i$  are chosen randomly to be either of the two choices of  $\phi_a$  and  $\phi_b$ . One of them (here  $\phi_b$ ) is attributed to two successive sites (so this model is called dimer). It is shown[39] that states at the resonant energy  $E = \phi_b$  are delocalized when  $-2t \leq \phi_a - \phi_b \leq 2t$ . In this study, we choose  $\phi_a = 0$ , so the condition is  $-2 \leq \phi_b \leq 2$ . States at energies other than the resonant energy are localized. The Anderson phase transition in this model has been studied before from different perspectives[36, 40–44].

Another model is the generalized Aubry-Andry model[45], where the on-site energies  $\varepsilon_i$  are:

$$\varepsilon_i = 2\lambda \frac{\cos(2\pi i b)}{1 - \alpha \cos(2\pi i b)}, \quad (4)$$

$b$  is an irrational number, and we set it to be the golden ratio  $b = \frac{1+\sqrt{5}}{2}$ . Since  $b$  is not a rational number, the system has incommensurate periodicity with respect to the lattice periodicity, which we set it to be 1. Thus, this system is neither completely periodic nor completely random.

This model has mobility edges separating delocalized and localized eigenstates at the following eigenenergy[45]:

$$E_{\text{mobility edge}} = 2s \operatorname{sgn}(\lambda) \frac{|t| - |\lambda|}{\alpha}. \quad (5)$$

One special case for this model is  $\alpha = 0$ , which is the Aubry-Andry model, with the following on-site energies:

$$\varepsilon_i = 2\lambda \cos(2\pi i b + \theta), \quad (6)$$

here, a random phase  $\theta$  is added which is distributed uniformly between  $-\pi$  and  $\pi$ . It is shown that for  $\lambda < 1$ , all states are delocalized and for  $\lambda > 1$ , all states are localized[17]. Thus, there is a phase transition between delocalized and localized phases at  $\lambda = 1$ . The properties of this model have been studied before[44, 46–48]. We should emphasize that all the models mentioned above, and their Anderson phase transition have been studied thoroughly before; here we just use them to verify our idea.

Since both models describe the free fermions, we deal with Hamiltonians that are represented by  $N \times N$  matrices. These matrices can be diagonalized numerically. In this paper, we use LAPACK[49] to diagonalize the matrices, and obtain their eigenvalues and eigenvectors.

In this paper, we want to consider the overlap of the state of the system with PBC and the state of the system with APBC. Here, we explain how to calculate the SPO and GSO overlaps. By PBC we mean  $c_{N+1}^\dagger = +c_1^\dagger$ , and by APBC we mean  $c_{N+1}^\dagger = -c_1^\dagger$ . If we assume the following free fermion Hamiltonians with PBC and APBC:

$$H_{\text{PBC}} = \sum_{i,j}^N h_{ij}^{\text{P}} c_i^\dagger c_j, \quad (7)$$

$$H_{\text{APBC}} = \sum_{i,j}^N h_{ij}^{\text{A}} c_i^\dagger c_j, \quad (8)$$

where,  $h^{\text{P}}$  and  $h^{\text{A}}$  can be determined by the choice of the on-site energies (RD, gAA, or AA model) and the boundary conditions (either PBC or APBC). We can diagonalize the matrix  $h$  in the

following way:

$$h^{\text{P}} = U E^{\text{P}} U^\dagger \quad (9)$$

$$h^{\text{A}} = V E^{\text{A}} V^\dagger, \quad (10)$$

and find the eigen-energies  $E$  as well as the single-particle eigenstates  $\psi$  for each Hamiltonian ( $\psi_i^{n,\text{PBC}} = U_{in}$  is the  $i$ th element of the  $n$ th eigenvector, and similarly for  $\psi_i^{n,\text{APBC}} = V_{in}$ ). To calculate the ground-state overlap, which is the overlap between ground-state of the Hamiltonian with the PBC ( $\psi_{MB}^{\text{PBC}}$ ) and APBC ( $\psi_{MB}^{\text{APBC}}$ ), we use the following method[30]. After diagonalization, we can write both Hamiltonians as:

$$H_{\text{PBC}} = \sum_{k=1}^N E_k^{\text{P}} b_k^\dagger b_k, \quad (11)$$

$$H_{\text{APBC}} = \sum_{k=1}^N E_k^{\text{A}} a_k^\dagger a_k, \quad (12)$$

where  $b_k^\dagger = \sum_i U_{ik} c_i^\dagger$ , and  $a_k^\dagger = \sum_i V_{ik} c_i^\dagger$ . Then, GSO is:

$$\begin{aligned} \text{GSO} &= |\langle \psi_{MB}^{\text{PBC}} | \psi_{MB}^{\text{APBC}} \rangle| \\ &= \left| \langle 0 | \prod_k^{N_F} b_k \prod_{k'}^{N_F} a_{k'}^\dagger | 0 \rangle \right| \\ &= |\det(B)| \end{aligned} \quad (13)$$

where  $B$  is a matrix built from the first  $N_F \times N_F$  part of the matrix  $U^\dagger V$  ( $N_F$  is the number of fermions).

We also use the notion of the single-particle overlap, which is the overlap between corresponding single-particle eigenstates of the Hamiltonian with PBC and with APBC. To calculate it, we dot product the single-particle eigenstate  $\psi_n^{\text{APBC}}$  with the corresponding eigenstate  $\psi_n^{\text{PBC}}$  for specific  $n$ th level. We consider only its absolute values:

$$\text{SPO} = |\langle \psi_n^{\text{PBC}} | \psi_n^{\text{APBC}} \rangle| \quad (14)$$

We note that there is randomness in the AA and RD models, and thus we take the disorder average of the above-mentioned GSO and SPO over different random realizations to obtain their mean values.

### 3 Results

In this section, we present the results of the numerical calculations. First, we will study the GSO for the above mentioned models. In the subsequent subsection, we present the results of the SPO and we explain its benefits over GSO for models with mobility edges.

#### 3.1 Ground-State Overlap

First we calculate the GSO for the RD model, we as we change the  $\phi_b$  and we always set  $E_F = \phi_b$ . The state of the system at  $E = E_F$  is delocalized for  $\phi_b < 2$ , and it is localized for  $\phi_b > 2$  (because of the mirror symmetry in this model, we only consider the positive part). The results are plotted in the Fig. 1 for different system sizes  $N$ . We can see that GSO has different behaviors in the delocalized and localized phases. In the delocalized phase ( $\phi_b < 2$ ), the GSO is smaller compared with that in the localized phase ( $\phi_b > 2$ ). We can also see that it approaches unity deep in the localized phase. It is evident that we can distinguish delocalized and localized phases from the behavior of the GSO near the phase transition point. We also calculate the GSO for the AA model. The results are plotted in Fig. 2. The behavior of the GSO for the AA model is not as sharp as the behavior of the RD model. But, still it is obvious that GSO approaches 1 in the localized phase ( $\lambda > 1$ ), and it is smaller in the delocalized phase, ( $\lambda < 1$ ).

#### 3.2 Single-Particle Overlap

To calculate the GSO for the AA and RD models, first we set a Fermi energy, and then based on the obtained number of fermions, we use Eq. (13). Based on the GSO, we saw that there is a distinction between delocalized and localized states for both models. let's look at the the entire spectrum in these models. We know that the AA model does not have mobility edges between delocalized and localized states. Either all the states are delocalized ( $\lambda < 1$ ) or all the states are localized ( $\lambda > 1$ ). In the RD model, only the single-particle eigenstate at the resonant energy is delocalized, and all the other states are localized. To distinguish between delocalized and localized *single-particle eigenstates*, we use the notion of the SPO. For both AA and RD models, we calculated the SPO. The numerical results are plotted in Fig. 3. For

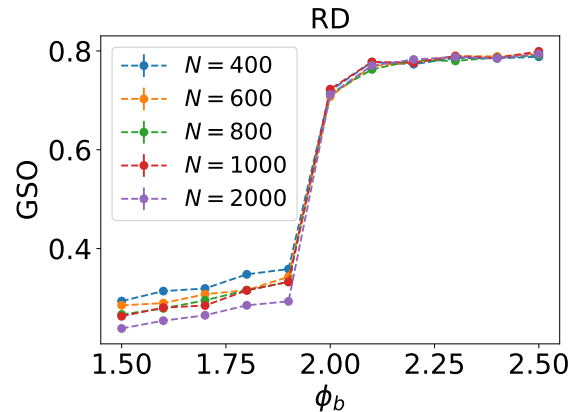


**Fig. 1** The overlap between the ground-state of the system with PBC and APBC, as we change  $\phi_b$  for the RD model. We set  $E_F = \phi_b$ . At each data point, the disorder average is taken over 2000 random realizations. Behavior of the GSO for this model is sharp at the phase transition point.

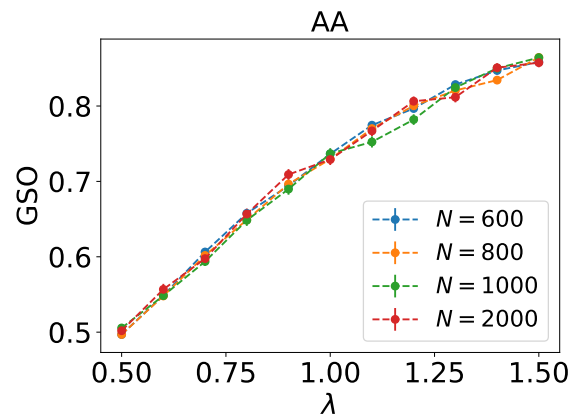


**Fig. 2** The overlap between the ground-state of the system with PBC and APBC, as we change  $\lambda$  for the AA model. The GSO is not as sharp as in the RD models. The overlaps approaches 1 in the localized phase ( $\lambda > 1$ ), and it gets smaller in the delocalized phase ( $\lambda < 1$ ). We set  $E_F = 0$ . At each data point, the disorder average is taken over 2000 random realizations.

the AA model with either *all* delocalized or *all* localized states, we see that SPO is very close to 1 (in the localized phase) or lower than 1 (in the delocalized phase). SPO for the RD model has more features. For the case of  $\phi_b = 3$ , where all states are localized, we see that SPO is 1 for the entire spectrum. On the other hand, for the  $\phi_b = 1$  where single-particle eigenstate at the resonant energy  $E = \phi_b = 1$  is delocalized and all the other single-particle eigenstates are localized,



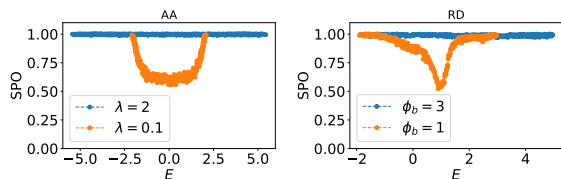


**Fig. 3** The single-particle overlap between the single-particle eigenstates with PBC and APBC for the entire spectrum. Left panel: SPO for the AA model. In the localized phase ( $\lambda = 2$ ) SPO is very close to 1 for the entire spectrum; in the delocalized phase ( $\lambda = 0.1$ ) SPO is lower than 1 for the entire spectrum. Right panel: SPO for the RD model. For  $\phi_b = 3$  where all single-particle eigenstates are localized, SPO is close to 1 for the entire spectrum. For the  $\phi_b = 1$  with a delocalized single-particle eigenstate at the  $E = 1$ , SPO for points close to this energy is lower than 1.

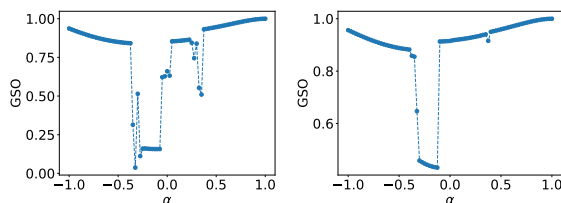


**Fig. 4** the ground-state overlap for the gAA model (Eq. (4)) as we change  $\alpha$  from  $-1$  to  $1$  and for two choices of  $\lambda = 0.9$  (left panel) and  $\lambda = -1.1$  (right panel). We set  $N = 500$ ,  $E_F = 0$ . Although this model has mobility edges, no information about them can be obtained from GSO plots. To see the mobility edges, we use SPO (see Fig. 5)

we see that SPO is smaller than 1 around the resonant energy, and it becomes close to 1 away from the resonant energy. Thus, the SPO can be used to characterize the *spectral resolution* of the system for delocalized-localized phase transition.

It gets more complicated if we consider models with mobility edges between delocalized and localized phases. One example would be the gAA model with on-site energies given by Eq. (4). This model has mobility edges (given by Eq. (5)) that separate delocalized and localized single-particle eigenstates. If we set the Fermi energy  $E_F = 0$  and obtain the GSO, we will obtain the plots in Fig. 4. It is evident that we can not locate the mobility edges from this plot.

However, the SPO exhibit the detailed features of the mobility edges. In Fig. 5, we plot the result of the SPO for the entire spectrum, for  $-1 \leq \alpha \leq 1$  and for two choices of  $\lambda = 0.9, -1.1$ . Categorization of the single-particle eigenstates based on the SPO is entirely in agreement with

the mobility edges given by Eq. (5). This shows that the SPO between single-particle eigenstates with PBC and APBC is an informative measure to characterize the single-particle delocalized and localized eigenstates.

## 4 conclusion

In this paper, we studied the effect of the boundary conditions on the overlap between the ground-state of the system with PBC and APBC. We observe that the overlap in the delocalized phase is smaller than the overlap in the localized phase, where it goes to unity. These observations stem from the fact that state of the system in the localized phase, does not change upon changing the boundary conditions. However, the single-particle eigenstate is affected by the change in the boundary conditions in the delocalized phase.

This conjecture enabled us to use the notion of the GSO to distinguish delocalized from localized phases. For the AA and RD models, we saw that GSO has distinguishing features in the delocalized and localized phases. In addition, we utilize the notion of the SPO, to characterize the single-particle mobility edges in models like gAA. This idea can also be used for characterizing other free fermion models with mobility edges that separate delocalized, localized, and also multifractal eigenstates[18, 50, 51]. It is also possible to generalize the notion of the SPO and GSO for many-body interacting models, although some effort has been done before[37].

## Data Availability Statement

The data-sets generated during and/or analyzed during the current study are available from the corresponding author on reasonable request.

## Author Contribution Statement

The conceptualization, numerical calculations, and writing made by the single author.

## acknowledgments

The author gratefully acknowledges the high performance computing center of the university of Mazandaran for providing computing resources and time.

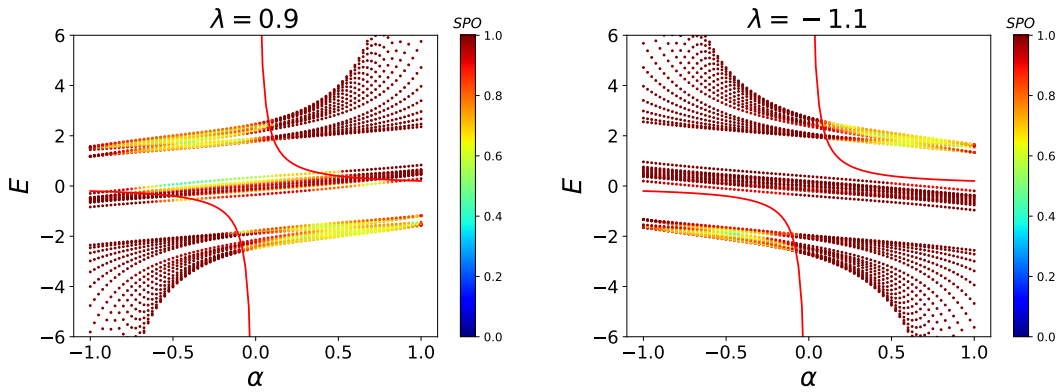


**Fig. 5** The single-particle overlap for the gAA model (Eq. (4)) for the entire spectrum of the Hamiltonian, as we change  $\alpha$  from  $-1$  to  $1$  and for two choices of  $\lambda = 0.9$  (left panel) and  $\lambda = -1.1$  (right panel). The red line is the mobility edges, separating delocalized and localized phases based on Eq. (5). Color bar shows the scale of the SPO. We set  $N = 500$ . In contrast to GSO (Fig. 4), we can locate the mobility edges by SPO.

## References

- [1] Anderson, P. W. Absence of diffusion in certain random lattices. *Phys. Rev.* **109**, 1492–1505 (1958). URL <https://link.aps.org/doi/10.1103/PhysRev.109.1492>. <https://doi.org/10.1103/PhysRev.109.1492>.
- [2] Lagendijk, A., Van Tiggelen, B. & Wiersma, D. S. Fifty years of anderson localization. *Phys. Today* **62** (8), 24–29 (2009).
- [3] Semeghini, G. *et al.* Measurement of the mobility edge for 3d anderson localization. *Nature Physics* **11** (7), 554–559 (2015).
- [4] Economou, E. N. & Cohen, M. H. Existence of mobility edges in anderson's model for random lattices. *Phys. Rev. B* **5**, 2931–2948 (1972). URL <https://link.aps.org/doi/10.1103/PhysRevB.5.2931>. <https://doi.org/10.1103/PhysRevB.5.2931>.
- [5] Evers, F. & Mirlin, A. D. Anderson transitions. *Rev. Mod. Phys.* **80**, 1355–1417 (2008). URL <https://link.aps.org/doi/10.1103/RevModPhys.80.1355>. <https://doi.org/10.1103/RevModPhys.80.1355>.
- [6] Markos, P. Numerical analysis of the anderson localization. *arXiv preprint cond-mat/0609580* (2006).
- [7] Markos, P. & Kramer, B. Statistical properties of the anderson transition numerical results. *Philosophical Magazine B* **68** (3), 357–379 (1993). URL <https://doi.org/10.1080/13642819308215292>. <https://doi.org/10.1080/13642819308215292>, <https://arxiv.org/abs/https://doi.org/10.1080/13642819308215292>.
- [8] Izrailev, F. M. & Krokhin, A. A. Localization and the mobility edge in one-dimensional potentials with correlated disorder. *Phys. Rev. Lett.* **82**, 4062–4065 (1999). URL <https://link.aps.org/doi/10.1103/PhysRevLett.82.4062>. <https://doi.org/10.1103/PhysRevLett.82.4062>.
- [9] Mirlin, A. D., Fyodorov, Y. V., Dittes, F.-M., Quezada, J. & Seligman, T. H. Transition from localized to extended eigenstates in the ensemble of power-law random banded matrices. *Physical Review E* **54** (4), 3221 (1996).
- [10] Einstein, A., Podolsky, B. & Rosen, N. Can quantum-mechanical description of physical reality be considered complete? *Phys. Rev.* **47**, 777–780 (1935). URL <https://link.aps.org/doi/10.1103/PhysRev.47.777>. <https://doi.org/10.1103/PhysRev.47.777>.

- [11] Raimond, J. M., Brune, M. & Haroche, S. Manipulating quantum entanglement with atoms and photons in a cavity. *Rev. Mod. Phys.* **73**, 565–582 (2001). URL <https://link.aps.org/doi/10.1103/RevModPhys.73.565>. <https://doi.org/10.1103/RevModPhys.73.565>.
- [12] Schrödinger, E. Discussion of probability relations between separated systems. *Mathematical Proceedings of the Cambridge Philosophical Society* **31** (4), 555–563 (1935). <https://doi.org/10.1017/S0305004100013554>.
- [13] Osterloh, A., Amico, L., Falci, G. & Fazio, R. Scaling of entanglement close to a quantum phase transition. *Nature* **416** (6881), 608–610 (2002). URL <https://doi.org/10.1038/416608a>. <https://doi.org/10.1038/416608a>.
- [14] Amico, L., Fazio, R., Osterloh, A. & Vedral, V. Entanglement in many-body systems. *Rev. Mod. Phys.* **80**, 517–576 (2008). URL <https://link.aps.org/doi/10.1103/RevModPhys.80.517>. <https://doi.org/10.1103/RevModPhys.80.517>.
- [15] Horodecki, R., Horodecki, P., Horodecki, M. & Horodecki, K. Quantum entanglement. *Rev. Mod. Phys.* **81**, 865–942 (2009). URL <https://link.aps.org/doi/10.1103/RevModPhys.81.865>. <https://doi.org/10.1103/RevModPhys.81.865>.
- [16] Shklovskii, B. I., Shapiro, B., Sears, B. R., Lambrianides, P. & Shore, H. B. Statistics of spectra of disordered systems near the metal-insulator transition. *Phys. Rev. B* **47**, 11487–11490 (1993). URL <https://link.aps.org/doi/10.1103/PhysRevB.47.11487>. <https://doi.org/10.1103/PhysRevB.47.11487>.
- [17] Aubry, S. & André, G. Analyticity breaking and anderson localization in incommensurate lattices. *Ann. Israel Phys. Soc* **3** (133), 18 (1980).
- [18] Deng, X., Ray, S., Sinha, S., Shlyapnikov, G. V. & Santos, L. One-dimensional quasicrystals with power-law hopping. *Phys. Rev. Lett.* **123**, 025301 (2019). URL <https://link.aps.org/doi/10.1103/PhysRevLett.123.025301>. <https://doi.org/10.1103/PhysRevLett.123.025301>.
- [19] Oganesyan, V. & Huse, D. A. Localization of interacting fermions at high temperature. *Phys. Rev. B* **75**, 155111 (2007). URL <https://link.aps.org/doi/10.1103/PhysRevB.75.155111>. <https://doi.org/10.1103/PhysRevB.75.155111>.
- [20] Atas, Y. Y., Bogomolny, E., Giraud, O. & Roux, G. Distribution of the ratio of consecutive level spacings in random matrix ensembles. *Phys. Rev. Lett.* **110**, 084101 (2013). URL <https://link.aps.org/doi/10.1103/PhysRevLett.110.084101>. <https://doi.org/10.1103/PhysRevLett.110.084101>.
- [21] Roy, N. & Sharma, A. Entanglement contour perspective for “strong area-law violation” in a disordered long-range hopping model. *Phys. Rev. B* **97**, 125116 (2018). URL <https://link.aps.org/doi/10.1103/PhysRevB.97.125116>. <https://doi.org/10.1103/PhysRevB.97.125116>.
- [22] Buonsante, P. & Vezzani, A. Ground-state fidelity and bipartite entanglement in the bose-hubbard model. *Phys. Rev. Lett.* **98**, 110601 (2007). URL <https://link.aps.org/doi/10.1103/PhysRevLett.98.110601>. <https://doi.org/10.1103/PhysRevLett.98.110601>.
- [23] Chen, S., Wang, L., Hao, Y. & Wang, Y. Intrinsic relation between ground-state fidelity and the characterization of a quantum phase transition. *Phys. Rev. A* **77**, 032111 (2008). URL <https://link.aps.org/doi/10.1103/PhysRevA.77.032111>. <https://doi.org/10.1103/PhysRevA.77.032111>.
- [24] Yang, M.-F. Ground-state fidelity in one-dimensional gapless models. *Phys. Rev. B* **76**, 180403 (2007). URL <https://link.aps.org/doi/10.1103/PhysRevB.76.180403>. <https://doi.org/10.1103/PhysRevB.76.180403>.
- [25] Rossini, D. & Vicari, E. Ground-state fidelity at first-order quantum transitions. *Phys. Rev. E* **98**, 062137 (2018). URL <https://link.aps.org/doi/10.1103/PhysRevE.98.062137>.



- 10.1103/PhysRevE.98.062137. <https://doi.org/10.1103/PhysRevE.98.062137> .
- [26] Zhao, J.-H. & Zhou, H.-Q. Singularities in ground-state fidelity and quantum phase transitions for the kitaev model. *Phys. Rev. B* **80**, 014403 (2009). URL <https://link.aps.org/doi/10.1103/PhysRevB.80.014403>. <https://doi.org/10.1103/PhysRevB.80.014403> .
- [27] Łącki, M., Damski, B. & Zakrzewski, J. Numerical studies of ground-state fidelity of the bose-hubbard model. *Phys. Rev. A* **89**, 033625 (2014). URL <https://link.aps.org/doi/10.1103/PhysRevA.89.033625>. <https://doi.org/10.1103/PhysRevA.89.033625> .
- [28] Anderson, P. W. Infrared catastrophe in fermi gases with local scattering potentials. *Phys. Rev. Lett.* **18**, 1049–1051 (1967). URL <https://link.aps.org/doi/10.1103/PhysRevLett.18.1049>. <https://doi.org/10.1103/PhysRevLett.18.1049> .
- [29] Vasseur, R. & Moore, J. E. Multifractal orthogonality catastrophe in one-dimensional random quantum critical points. *Phys. Rev. B* **92**, 054203 (2015). URL <https://link.aps.org/doi/10.1103/PhysRevB.92.054203>. <https://doi.org/10.1103/PhysRevB.92.054203> .
- [30] Deng, D.-L., Pixley, J. H., Li, X. & Das Sarma, S. Exponential orthogonality catastrophe in single-particle and many-body localized systems. *Phys. Rev. B* **92**, 220201 (2015). URL <https://link.aps.org/doi/10.1103/PhysRevB.92.220201>. <https://doi.org/10.1103/PhysRevB.92.220201> .
- [31] Cosco, F. *et al.* Statistics of orthogonality catastrophe events in localised disordered lattices. *New Journal of Physics* **20** (7), 073041 (2018). URL <https://doi.org/10.1088/1367-2630/aad10b>. <https://doi.org/10.1088/1367-2630/aad10b> .
- [32] Tonielli, F., Fazio, R., Diehl, S. & Marino, J. Orthogonality catastrophe in dissipative quantum many-body systems. *Phys. Rev. Lett.* **122**, 040604 (2019). URL <https://link.aps.org/doi/10.1103/PhysRevLett.122.040604>. <https://doi.org/10.1103/PhysRevLett.122.040604> .
- [33] Levine, G. C. Entanglement entropy in a boundary impurity model. *Phys. Rev. Lett.* **93**, 266402 (2004). URL <https://link.aps.org/doi/10.1103/PhysRevLett.93.266402>. <https://doi.org/10.1103/PhysRevLett.93.266402> .
- [34] Peschel, I. Entanglement entropy with interface defects. *Journal of Physics A: Mathematical and General* **38** (20), 4327–4335 (2005). URL <https://doi.org/10.1088/0305-4470/38/20/002>. <https://doi.org/10.1088/0305-4470/38/20/002> .
- [35] Edwards, J. T. & Thouless, D. J. Numerical studies of localization in disordered systems. *Journal of Physics C: Solid State Physics* **5** (8), 807–820 (1972). URL <https://doi.org/10.1088%2F0022-3719%2F5%2F8%2F007>. <https://doi.org/10.1088/0022-3719/5/8/007> .
- [36] Mohammad, P. & Montakhab, A. Sensitivity of the entanglement spectrum to boundary conditions as a characterization of the phase transition from delocalization to localization. *Phys. Rev. B* **96**, 045123 (2017). URL <https://link.aps.org/doi/10.1103/PhysRevB.96.045123>. <https://doi.org/10.1103/PhysRevB.96.045123> .
- [37] Pouranvari, M. & Liou, S.-F. Characterizing many-body localization via state sensitivity to boundary conditions. *Phys. Rev. B* **103**, 035136 (2021). URL <https://link.aps.org/doi/10.1103/PhysRevB.103.035136>. <https://doi.org/10.1103/PhysRevB.103.035136> .
- [38] Hashimoto, K. *et al.* Quantum hall transition in real space: From localized to extended states. *Phys. Rev. Lett.* **101**, 256802 (2008). URL <https://link.aps.org/doi/10.1103/PhysRevLett.101.256802>. <https://doi.org/10.1103/PhysRevLett.101.256802> .
- [39] Dunlap, D. H., Wu, H.-L. & Phillips, P. W. Absence of localization in a random-dimer model. *Phys. Rev. Lett.* **65**, 88–91

- (1990). URL <https://link.aps.org/doi/10.1103/PhysRevLett.65.88>. <https://doi.org/10.1103/PhysRevLett.65.88> .
- [40] Bovier, A. Perturbation theory for the random dimer model. *Journal of Physics A: Mathematical and General* **25** (5), 1021–1029 (1992). URL <https://doi.org/10.1088/0305-4470/25/5/011>. <https://doi.org/10.1088/0305-4470/25/5/011> .
- [41] Sedrakyan, T. Localization-delocalization transition in a presence of correlated disorder: The random dimer model. *Phys. Rev. B* **69**, 085109 (2004). URL <https://link.aps.org/doi/10.1103/PhysRevB.69.085109>. <https://doi.org/10.1103/PhysRevB.69.085109> .
- [42] Datta, P. K., Giri, D. & Kundu, K. Nature of states in a random-dimer model: Bandwidth-scaling analysis. *Phys. Rev. B* **48**, 16347–16356 (1993). URL <https://link.aps.org/doi/10.1103/PhysRevB.48.16347>. <https://doi.org/10.1103/PhysRevB.48.16347> .
- [43] Farchioni, R. & Grosso, G. Electronic transport for random dimer-trimer model hamiltonians. *Phys. Rev. B* **56**, 1170–1174 (1997). URL <https://link.aps.org/doi/10.1103/PhysRevB.56.1170>. <https://doi.org/10.1103/PhysRevB.56.1170> .
- [44] Pouranvari, M. & Abouie, J. Entanglement conductance as a characterization of a delocalized-localized phase transition in free fermion models. *Phys. Rev. B* **100**, 195109 (2019). URL <https://link.aps.org/doi/10.1103/PhysRevB.100.195109>. <https://doi.org/10.1103/PhysRevB.100.195109> .
- [45] Ganeshan, S., Pixley, J. H. & Das Sarma, S. Nearest neighbor tight binding models with an exact mobility edge in one dimension. *Phys. Rev. Lett.* **114**, 146601 (2015). URL <https://link.aps.org/doi/10.1103/PhysRevLett.114.146601>. <https://doi.org/10.1103/PhysRevLett.114.146601> .
- [46] Domínguez-Castro, G. A. & Paredes, R. The aubry–andré model as a hobbyhorse for understanding the localization phenomenon. *European Journal of Physics* **40** (4), 045403 (2019). URL <https://doi.org/10.1088/1361-6404/ab1670>. <https://doi.org/10.1088/1361-6404/ab1670> .
- [47] Cookmeyer, T., Motruk, J. & Moore, J. E. Critical properties of the ground-state localization-delocalization transition in the many-particle aubry–andré model. *Phys. Rev. B* **101**, 174203 (2020). URL <https://link.aps.org/doi/10.1103/PhysRevB.101.174203>. <https://doi.org/10.1103/PhysRevB.101.174203> .
- [48] Riddell, J. & Sørensen, E. S. Out-of-time-order correlations in the quasiperiodic aubry–andré model. *Phys. Rev. B* **101**, 024202 (2020). URL <https://link.aps.org/doi/10.1103/PhysRevB.101.024202>. <https://doi.org/10.1103/PhysRevB.101.024202> .
- [49] Anderson, E. *et al.* *LAPACK Users' Guide* Third edn (Society for Industrial and Applied Mathematics, Philadelphia, PA, 1999).
- [50] Fraxanet, J., Bhattacharya, U., Grass, T., Lewenstein, M. & Dauphin, A. Localization and multifractal properties of the long-range kitaev chain in the presence of an aubry–andré–harper modulation (2022). [2201.05458](https://arxiv.org/abs/2201.05458).
- [51] Biddle, J., Priour, D. J., Wang, B. & Das Sarma, S. Localization in one-dimensional lattices with non-nearest-neighbor hopping: Generalized anderson and aubry–andré models. *Phys. Rev. B* **83**, 075105 (2011). URL <https://link.aps.org/doi/10.1103/PhysRevB.83.075105>. <https://doi.org/10.1103/PhysRevB.83.075105> .